Harnessing Ferroptosis in PDAC: Curcumin Enhances RSL3-Induced Lipid Peroxidation and Cytotoxicity

Jonathan Song & Johnny Yi

Abstract

Pancreatic ductal adenocarcinoma (PDAC) is a highly lethal cancer that remains without an effective treatment and characterized by its resistance to conventional therapies and evasion of programmed cell death pathways. This study investigates a combinatorial therapeutic approach using curcumin, a natural ingredient with antioxidant properties, and RSL3, a ferroptosis inducer that inhibits GPX4 of the ASCL4 pathway. Mouse PDAC cells were treated with curcumin, RSL3, and Ferrostatin-1 both individually and in combination to determine their half-maximal inhibitory concentrations (IC50) and evaluate synergistic effects on cell viability. The IC50 of curcumin was found to be about 50 µM meanwhile for RSL3 it was about 0.5 µM. Dose-response assays revealed a possible enhanced cytotoxicity in combinatorial treatments compared to monotherapy, particularly with curcumin and RSL3. ROS staining using DCFH-DA was performed to visualize oxidative stress to physically see the ASCL4 pathway, although fixed-cell imaging introduced an unexpected result where a green-fluorescent ROS stain turned into a red nucleolus stain. Despite limitations including single-trial IC50 determinations and possible pipetting errors, our results suggest that curcumin primes PDAC cells for ferroptotic death enhancing RSL3 efficacy. These findings highlight the therapeutic potential of natural-drug combinations to treat PDAC.

Introduction

Pancreatic cancer remains as one of the deadliest forms of cancer, with a 5-year survival rate of only about 12% (Siegel *et al.*, 2024). Among pancreatic cancers, pancreatic ductal adenocarcinoma (PDAC) is responsible for over 90% of cases and is hard to treat due to its metastasis ability and resistance to conventional therapies (Zhang *et al.*, 2018). Pancreatic cancer is the third leading cause of cancer-related death with an estimated 62,200 new diagnoses in the US alone yearly (Stoffel *et al.*, 2023). Even with current standard treatments such as gemcitabine and FOLFIRINOX, PDAC remains one of the hardest cancers for these drugs to target (Valsechi *et al.*, 2013). Despite progress in chemotherapy, PDAC remains one of the deadliest cancers because it naturally resists cell death (Siegel *et al.*, 2024).

PDAC cells are unique in their ability to adapt to different environments that promote survival under harsh conditions, including dysregulated redox homeostasis, altered iron metabolism, and evasion of programmed cell death (PCD) pathways such as apoptosis (Gorrini *et al.*, 2013). An alternative approach that many scientists have begun researching is ferroptosis. This PCD pathway focuses on an iron-dependent form of regulated cell death driven by lipid peroxidation.

Lipid peroxidation is the process where reactive molecules, such as free radicals, attack lipids with carbon-carbon double bonds, mainly polyunsaturated fatty acids (PUFAs) (Ayala *et al.*, 2014). This leads to the formation of harmful compounds like lipid peroxyl radicals and hydroperoxides which ends up damaging other important membrane lipids causing cell death also known as ferroptosis. Ferroptosis bypasses traditional apoptotic resistance making it an effective form of treatment for PDAC cancer cells (Dixon *et al.*, 2012). However, inducing ferroptosis in PDAC remains challenging due to the cell's natural antioxidant mechanisms, such as the glutathione (GSH)-dependent system and upregulation of GPX4 (Yang *et al.*, 2014).

Figures 1-3 shows the ACSL4 pathway in PDAC cells. From literature review, this is one of the ferroptosis pathways that the three drugs we are using all play a role in (Sun *et al.*, 2023; Zhou *et al.*, 2024; Jiang *et al.*, 2024). Figure 1 shows that curcumin is not a direct inducer or inhibitor of this pathway but rather causes cell stress which creates ROS. In previous studies, curcumin has shown potential in reducing glutathione (GSH) levels, potentially by inhibiting upstream enzymes like γ-glutamylcysteine ligase (GCL) (Jiang *et al.*, 2024). Figure 2 shows that RSL3 directly inhibits the enzyme GPX4 which uses GSH, an antioxidant to detoxify oxidized lipids to prevent lipid peroxidation. Figure 3 shows that Ferrostatin-1 helps stop ferroptosis by removing ROS before they can target membrane lipids that cause lipid peroxidation. All three drugs play inducing or inhibiting effects on the ACSL4 pathway.
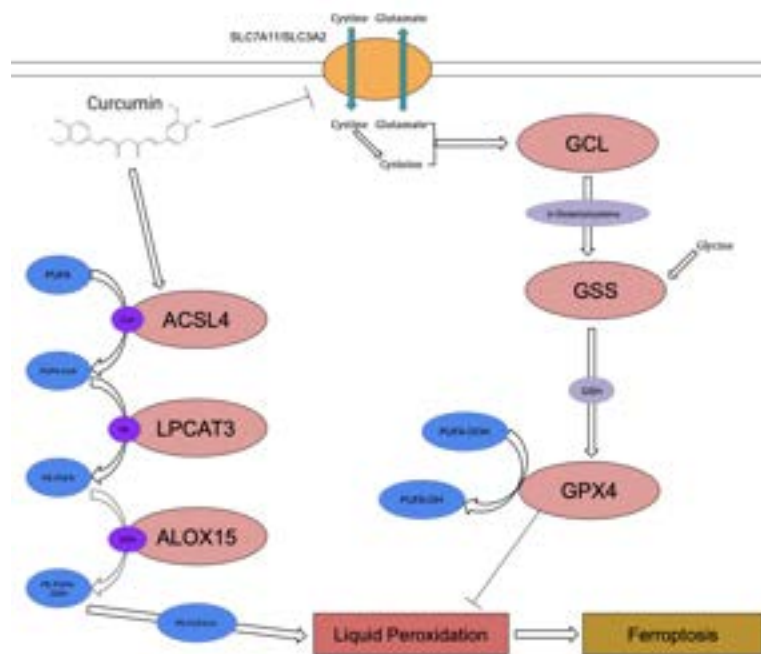

Figure 1. Diagram of ferroptosis induction pathway targeted by curcumin in PDAC cells. Curcumin (yellow) disrupts the cystine/glutamate antiporter (SLC7A11/SLC3A2), inhibiting glutathione (GSH) synthesis by suppressing γ-glutamylcysteine ligase (GCL) and glutathione

synthetase (GSS). This depletion of GSH (red) primes cells for RSL3 (blue)-mediated GPX4 inhibition, preventing the reduction of lipid peroxides (PE-PUFA-OOH). Concurrently, curcumin upregulates pro-ferroptotic factors (left) including LPCAT3 (lipid remodeling) and ALOX15 (lipid peroxidation), while suppressing c-Myc (not shown) to disable antioxidant defenses.
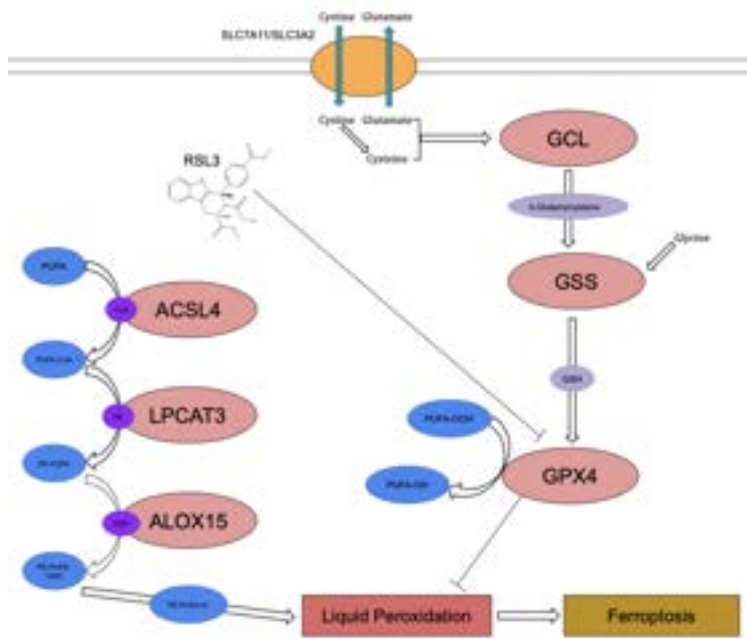

Figure 2. Mechanism of RSL3-induced ferroptosis in PDAC cells. RSL3 directly inhibits GPX4, blocking its ability to reduce lipid hydroperoxides (PUFA-OOH and PE-PUFA-OOH). This leads to: (1) accumulation of oxidized phospholipids (PE-PUFA-O•) through ALOX15-mediated peroxidation of polyunsaturated fatty acid (PUFA)-containing phospholipids (PE-PUFA), and (2) propagation of lipid radicals (PUFA-O•) that damage cellular membranes. The cystine/glutamate antiporter (SLC7A11/SLC3A2) maintains basal glutathione (GSH) levels, but RSL3's GPX4 inhibition renders this antioxidant system ineffective against lipid peroxidation, ultimately triggering ferroptotic cell death.
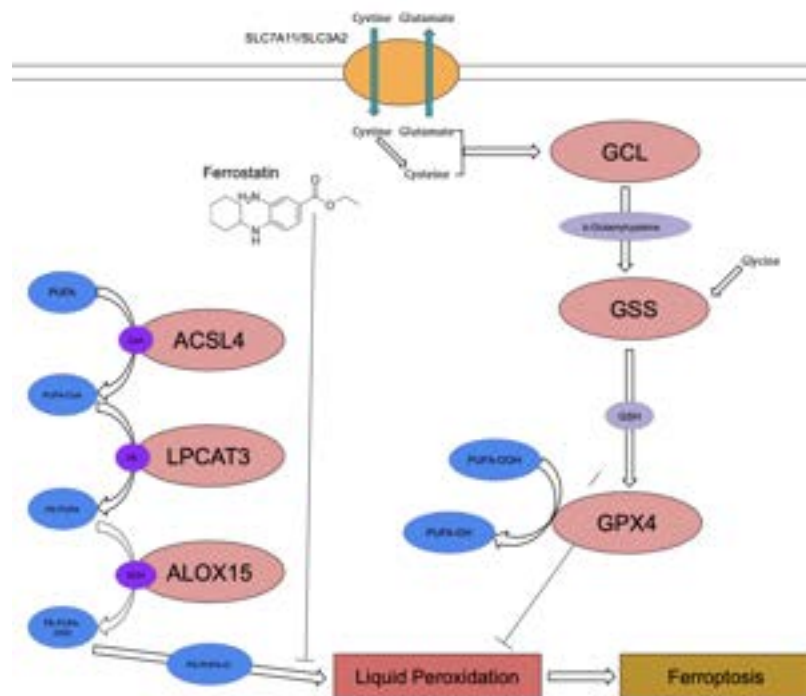
Figure 3. Ferrostatin-1 (Fer-1) rescues PDAC cells from RSL3-induced ferroptosis by blocking lipid peroxidation. Fer-1 acts as a radical-trapping antioxidant (RTA), directly neutralizing lipid radicals (PUFA-O•) and preventing their propagation along membranes. This inhibits the oxidation of phospholipid-bound polyunsaturated fatty acids (PE-PUFA-OOH → PE-PUFA-O•), effectively reversing RSL3-mediated ferroptotic cell death. While RSL3 (red) inactivates GPX4, leading to lethal lipid peroxide accumulation, Fer-1 provides an alternative protective mechanism independent of the GPX4/GSH axis.

Combinatorial drug approaches is an emerging strategy in oncology that helps address cancer resistance to typical mono-therapeutic drugs. Unlike monotherapies that often fail due to tumor adaptability, drug combinations can simultaneously target multiple pathways, creating a synergetic effect on killing cancerous cells while reducing their likelihood of resisting these therapies (Al-Lazikani *et al.*, 2012). This strategy is especially useful in aggressive cancers like PDAC, where tumor diversity due to mutations, metastatic potential, and a dense desmophilia microenvironment all help provide ways for the cancer cells to survive normal treatments (Sarantis *et al.*, 2020). Effective combinations typically follow one of three design principles: (1) vertical inhibition of signaling cascades, (2) horizontal blockade of parallel pathways, or (3) mechanistic synergy where one drug enables another's activity (Yesilkanal *et al.*, 2021). In our study, we investigated the third principle, focusing on whether curcumin exerts a synergistic effect in enhancing RSL3-induced ferroptosis.

As illustrated in Figure 4, the combination of curcumin and RSL3 appears to have a potential synergistic effect in promoting ferroptosis in PDAC cells. This dual treatment likely disrupts

redox homeostasis and enhances lipid peroxidation, culminating in ferroptotic cell death. The addition of Ferrostatin-1 in the experimental setup is to confirm the specificity of this cell death pathway, as its protective effects against RSL3-induced cytotoxicity suggest that the observed cell death is ferroptotic in nature.

The potential of ferroptosis as a therapeutic strategy in PDAC is increasingly recognized, offering a promising new form of treatment for targeting apoptosis-resistant tumors (Lopez-Blazquez *et al.*, 2023). Such strategies, which have shown success in other cancers, may prove to be a more effective treatment towards PDAC. RLS3 has proven to promote ferroptosis in colorectal cancer cell lines (Sui *et al.*, 2018). In breast cancer cell lines, RSL3 has shown to enhance the sensitivity of multidrug-resistant tumors to chemotherapeutics while also promoting lipid-peroxidation (Perera *et al.*, 2025). In triple-negative breast cancer, it was proven that RSL3 induced ferroptosis and suggested that it has potential in combinatorial approaches (Yuan *et al.*, 2025). Curcumin through literature review also had significant potential in promoting ferroptosis like in colorectal cancer (Guo *et al.*, 2024), Hepatocellular carcinoma (Jiang *et al.*, 2024), and Non–small-cell lung cancer (Tang *et al.*, 2021).

However, reviewing existing literature, we found no prior studies investigating the combinatorial use of curcumin and RSL3 in the context of inducing ferroptosis. While both agents have been individually studied for their roles in triggering cell death pathways, the potential synergistic interaction between the two has not yet been explored. This lack of precedent shows a critical gap in current research and proves the need and significance of our investigation.
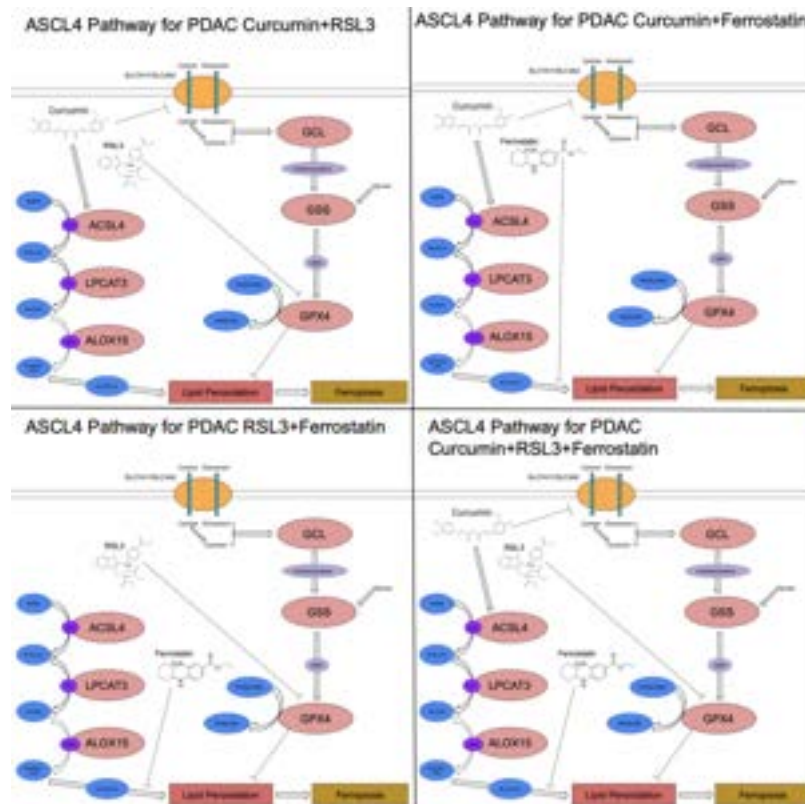
Figure 4. Proposed ferroptotic mechanisms for drug combinations of curcumin, RSL3, and ferrostatin-1 in PDAC cells. Curcumin + RSL3 (Top Left), Curcumin + Ferrostatin-1 (Top Right), RSL3 + Ferrostatin(Bottom Left), Curcumin + RSL3 + Ferrostatin(Bottom Right).

Materials & Methods

Figure 5 outlines the general procedure for the cell viability assays we conducted, highlighting each major step in the order they were performed. It can be used to summarize our main procedure in our cell viability assay. These assays were performed to understand how effective each drug was at killing PDAC cells.
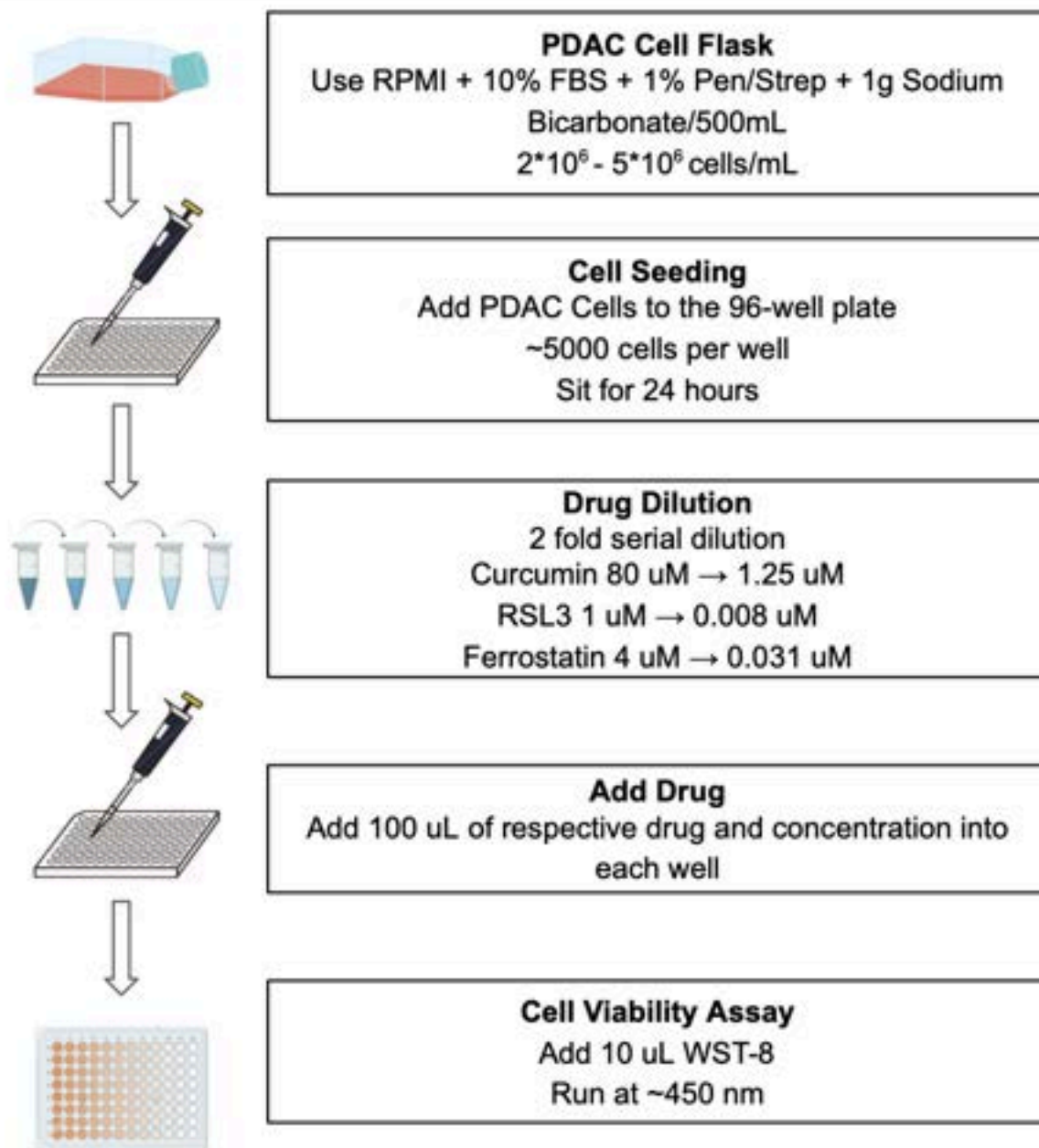
PDAC Cell Flask
Use RPMI + 10% FBS + 1% Pen/Strep + 1g Sodium
Bicarbonate/500mL
$2*10^6 - 5*10^6$ cells/mL

Cell Seeding
Add PDAC Cells to the 96-well plate
~5000 cells per well
Sit for 24 hours

Drug Dilution
2 fold serial dilution
Curcumin 80 uM → 1.25 uM
RSL3 1 uM → 0.008 uM
Ferrostatin 4 uM → 0.031 uM

Add Drug
Add 100 uL of respective drug and concentration into
each well

Cell Viability Assay
Add 10 uL WST-8
Run at ~450 nm

Figure 5. Workflow for PDAC Cell Viability Assay. The process begins with culturing PDAC cells in RPMI medium supplemented with 10% FBS, 1% Pen/Strep, and 1 g Sodium Bicarbonate/500 mL at a density of $2×10^6$ - $5×10^6$ cells/mL. Cells are then seeded into a 96-well plate at 5000 cells per well and incubated for 24 hours. Drug dilution is performed via 2-fold serial dilution, preparing concentrations of Curcumin (80 μM → 1.25 μM), RSL3 (1 μM → 0.008 μM), and Ferrostatin (4 μM → 0.031 μM). Subsequently, 100 μL of each drug concentration is added to the respective wells where we wait 48 hours. Finally, cell viability is assessed by adding 10 μL WST-8 and measuring absorbance at ~450 nm. These same steps are used for combination drug trials however the only variance being the drug concentrations we are adding to each well.

Mouse pancreatic ductal adenocarcinoma (PDAC) cells were cultured in RPMI-1640 growth medium supplemented with 10% fetal bovine serum (FBS), 1% penicillin-streptomycin (Pen/Strep), and 1 g sodium bicarbonate per 500 mL of medium. Cells were maintained at 37°C in a humidified atmosphere with 5% CO_2. Subculturing was performed at 70-80% confluence using standard trypsinization procedures for epithelial cells. Cell counts were determined using a Countess automated cell counter prior to seeding of the cells.

Stock solutions of all compounds were prepared in dimethyl sulfoxide (DMSO). We started with 5 grams of curcumin while only 1 mg of RSL3 and Ferrostatin-1. We needed a 20 mM stock of curcumin, 10 mM stock of RSL3, and 10 mM stock of Ferrostatin-1. Calculations for our stock concentrations are below. All stock solutions were aliquoted and stored at -20°C protected from light.

Curcumin Equation
$$\text{Volume of DMSO (L)} = \frac{\text{Mass of Curcumin (g)}}{\text{Molar mass (g/mol)} \times \text{Desired concentration (mol/L)}}$$
$$\text{Volume of DMSO} = \frac{5 \text{ g}}{368.38 \text{ g/mol} \times 0.020 \text{ mol/L}} = \frac{5 \text{ g}}{7.3676 \text{ g/L}} \approx 0.6786 \text{ L}$$ $$\text{Volume of DMSO} \approx 678.6 \text{ mL}$$

RSL3 Equation
$$\text{Volume of DMSO (L)} = \frac{\text{Mass of RSL3 (g)}}{\text{Molar mass (g/mol)} \times \text{Desired concentration (mol/L)}}$$
$$\text{Volume of DMSO} = \frac{0.001 \text{ g}}{440.88 \text{ g/mol} \times 0.010 \text{ mol/L}} = \frac{0.001 \text{ g}}{4.4088 \text{ g/L}} \approx 0.0002268 \text{ L}$$ $$\text{Volume of DMSO} \approx 226.8 \text{ } \mu L$$

Ferrostatin-1 Equation
$$\text{Volume of DMSO (L)} = \frac{\text{Mass of Ferrostatin-1 (g)}}{\text{Molar mass (g/mol)} \times \text{Desired concentration (mol/L)}}$$
$$\text{Volume of DMSO} = \frac{0.001 \text{ g}}{262.35 \text{ g/mol} \times 0.010 \text{ mol/L}} = \frac{0.001 \text{ g}}{2.6235 \text{ g/L}} \approx 0.0003812 \text{ L}$$ $$\text{Volume of DMSO} \approx 381.2 \text{ } \mu L$$

Serial dilutions of all compounds were prepared on the day of treatment. For curcumin, nine 1.5 mL microcentrifuge tubes were labeled numerically from 1-9. The first tube was filled with

800 µL of a 40 µM curcumin solution, prepared by diluting the 20 mM stock. Tubes 2-8 each contained 400 µL of RPMI medium. A 400 µL aliquot was transferred from tube 1 to tube 2 and mixed thoroughly, with this serial dilution process repeated through tube 8. Tube 9 served as a media-only control. This procedure generated concentrations ranging from 40 µM to 0.3125 µM in half-log increments from tubes 1-8 with tube 9 holding 0 µM.

RSL3 dilutions followed an identical protocol but began with a 1 µM starting concentration, producing a range from 1 µM to 0.0078 µM with tube 9 holding 0 µM. Ferrostatin-1 dilutions started at 4 µM, yielding concentrations from 4 µM to 0.03125 µM with tube 9 holding 0 µM. Table 1 shows all the mono-therapeutic drug serial dilutions. All drug dilutions were prepared in RPMI medium supplemented with 10% FBS and 1% Pen/Strep, while trying to limit DMSO concentrations as it is known to kill cells.

Table 1. Two fold serial drug dilutions for mono-therapy trial showing the individual concentrations we used for curcumin, RSL3, and Ferrostatin-1 in each well

Curcumin

Final Conc (µM)	Stock (µL)	DMEM (µL)
40.000	400	400
20.000	400	400
10.000	400	400
5.000	400	400
2.500	400	400
1.250	400	400
0.625	400	400
0.3125	400	400

RSL3

Final Conc (µM)	Stock (µL)	DMEM (µL)
1.000	400	400
0.500	400	400
0.250	400	400
0.125	400	400
0.0625	400	400
0.03125	400	400
0.01563	400	400
0.00781	400	400

Ferrostatin-1

Final Conc (µM)	Stock (µL)	DMEM (µL)
4.000	400	400
2.000	400	400
1.000	400	400
0.500	400	400
0.250	400	400
0.125	400	400
0.0625	400	400
0.03125	400	400

Cells were seeded in 96-well plates with a systematically arranged layout for the treatment conditions. As shown in Table 2, columns 2-9 contained the dilution series (highest to lowest concentration), while columns 10-11 served as controls. Rows B-D housed curcumin treatments (40 µM to 0.3125 µM), rows E-G contained RSL3 dilutions (1 µM to 0.0078 µM), and rows B-D of a second plate held Ferrostatin-1 concentrations (4 µM to 0.03125 µM). Each condition was replicated in triplicate wells to ensure statistical robustness.

Table 2. 96-well plate set up for the mono-therapy drug trial and their respective drug concentration in each well with curcumin and RSL3 shown in plate 1 meanwhile Ferrostatin-1 shown in plate 2

Curcumin and RSL3 Plate

	1	2	3	4	5	6	7	8	9	10	11	12
A												
B		Cur 40 uM	Cur 20 uM	Cur 10 uM	Cur 5 uM	Cur 2.5 uM	Cur 1.25 uM	Cur 0.63 uM	Cur 0.31 uM	CNTRL		
C		Cur 40 uM	Cur 20 uM	Cur 10 uM	Cur 5 uM	Cur 2.5 uM	Cur 1.25 uM	Cur 0.63 uM	Cur 0.31 uM	CNTRL		
D		Cur 40 uM	Cur 20 uM	Cur 10 uM	Cur 5 uM	Cur 2.5 uM	Cur 1.25 uM	Cur 0.63 uM	Cur 0.31 uM	CNTRL		
E		R 1 uM	R 0.5 uM	R 0.25 uM	R 0.125 uM	R 0.063 uM	R 0.031 5 uM	R 0.016 5 uM	R 0.008 uM	CNTRL		
F		R 1 uM	R 0.5 uM	R 0.25 uM	R 0.125 uM	R 0.063 uM	R 0.031 5 uM	R 0.016 uM	R 0.008 uM	CNTRL		
G		R 1 uM	R 0.5 uM	R 0.25 uM	R 0.125 uM	R 0.063 uM	R 0.031 5 uM	R 0.016 uM	R 0.008 uM	CNTRL		
H												

Ferrostatin Plate

	1	2	3	4	5	6	7	8	9	10	11	12
A												
B		F 4 uM	F 2 uM	F 1 uM	F .5 uM	F .25 uM	F .125 uM	F .063 uM	F .031 uM	CNTRL		
C		F 4 uM	F 2 uM	F 1 uM	F .5 uM	F .25 uM	F .125 uM	F .063 uM	F .031 uM	CNTRL		
D		F 4 uM	F 2 uM	F 1 uM	F .5 uM	F .25 uM	F .125 uM	F .063 uM	F .031 uM	CNTRL		
E												
F												
G												
H												

Following 24-hour cell attachment, media was carefully removed and replaced with 100 µL of the respective treatment solution for each well. Two columns of control wells were created in addition to the eight 2-fold dilution series. Each plate included multiple control types: column 10 contained untreated cell controls, column 11 held media only which served as a reference for plate normalization. This comprehensive control scheme enabled accurate background subtraction and normalization during data analysis. Plates were incubated under standard conditions (37°C, 5% CO2) for 48 hours before viability assessment.

To determine cell viability, we used a WST-8 assay. We added 10 µL of reagent to each well and incubated for 1.5 hours at 37°C. Absorbance was measured at 450 nm using a microplate reader. When we got absorbance we normalized all the values as shown by the calculation below.

$$\text{Normalized Viability (\%)} = \left(\frac{A_{\text{sample}} - A_{\text{media only}}}{A_{\text{cell control}} - A_{\text{media only}}} \right) \times 100\%$$

After determining the IC50 values from monotherapy experiments and comparing them to literature, we used these concentrations to prepare individual drug treatments for ROS staining, comparing treated PDAC cells to untreated controls. PDAC cells were cultured on rectangular coverslips and allowed to adhere for 24 hours. They were then treated with curcumin (50 µM), RSL3 (0.5 µM), or ferrostatin-1 (4 µM) individually and incubated for 48 hours. Following treatment, cells were stained with 10 µM 2′,7′-dichlorofluorescein diacetate (DCFH-DA) and

DAPI for fluorescent microscopy. The DCFH-DA concentration was selected based on previously established protocols for ROS detection in PDAC cells (Kim & Xue, 2021).

From monotherapy assay results, combination drug treatment cell viability assays were also conducted, but with different initial drug concentrations. Due to an error, the drugs were diluted 7 times instead of 8. The starting concentrations of each drug were also increased to observe stronger effects. The starting concentrations for Curcumin, RSL3, and Ferrostatin-1 were altered from 40 µM, 1 µM, and 4 µM to 80 µM, 4 µM, and 8 µM, respectively. Note that the concentrations of each two fold dilution remains the same even in combined drug solutions in order to maintain consistency. Table 3 shows us the serial dilution we did for drug combinations.

Table 3. Two fold serial drug dilutions for drug combination trial showing the concentrations of each drug in the combination trial we used for curcumin+RSL3, curcumin+Ferrostatin-1, RSL3+Ferrostatin-1, and curcumin+RSL3+Ferrostatin-1 in each well

Curcumin + RSL3

Dilution	Curcumin Conc (µM)	RSL3 Conc (µM)	Total Volume Including Media (µL)
1×	80	4	800
1/2×	40	2	800
1/4×	20	1	800
1/8×	10	0.5	800
1/16×	5	0.25	800
1/32×	2.5	0.13	800
1/64×	1.25	0.06	800
0×	0	0	800

Curcumin + Ferrostatin

Dilution	Curcumin Conc (µM)	Ferrostatin Conc (µM)	Total Volume Including Media (µL)
1×	80	8	800
1/2×	40	4	800
1/4×	20	2	800
1/8×	10	1	800
1/16×	5	0.5	800
1/32×	2.5	0.25	800
1/64×	1.25	0.13	800
0×	0	0	800

RSL3 + Ferrostatin

Dilution	RSL3 Conc (µM)	Ferrostatin Conc (µM)	Total Volume Including Media (µL)
1×	4	8	800
1/2×	2	4	800
1/4×	1	2	800
1/8×	0.5	1	800
1/16×	0.25	0.5	800
1/32×	0.13	0.25	800
1/64×	0.06	0.13	800
0×	0	0	800

Curcumin + RSL3 + Ferrostatin

Dilution	Curcumin Conc (µM)	RSL3 Conc (µM)	Ferrostatin Conc (µM)	Total Volume Including Media (µL)
1×	80	4	8	800
1/2×	40	2	4	800
1/4×	20	1	2	800
1/8×	10	0.5	1	800
1/16×	5	0.25	0.5	800
1/32×	2.5	0.13	0.25	800
1/64×	1.25	0.06	0.13	800
0×	0	0	0	800

We conducted an additional trial with curcumin to explore a potential trend we had observed, using a two-fold serial dilution starting at 80 µM and decreasing down to 1.25 µM. Table 4 shows the serial dilution table we did for this second trail of Curcumin.

Table 4. Second trial of curcumin with another two fold serial drug dilutions for mono-therapy trial showing the concentrations of curcumin in each well

Curcumin 2

Final Conc (μM)	Stock (μL)	DMEM (μL)
80.000	400	400
20.000	400	400
20.000	400	400
10.000	400	400
5.000	400	400
2.500	400	400
1.250	400	400
0	400	400

Once again, cells were seeded in 96-well plates with a systematically arranged layout for the treatment conditions. Table 5 shows that columns 2-8 contained the dilution series (highest to lowest concentration), while columns 9-10 served as controls. For this new trial, we used 3 96-well plates. In our first plate, rows B-D housed curcumin+RSL3 treatments while rows E-G contained curcumin+Ferrostatin-1 dilutions. In our second plate, rows B-D of a second plate held RSL3+Ferrostatin-1 treatments while rows E-G contained curcumin+RSL3+Ferrostatin-1 dilutions. Lastly, our third plate held our second trial of only curcumin being located in rows B-D. Each condition was replicated in triplicate wells to ensure statistical robustness.

Table 5. 96-well plate set up for the combination drug trial and their respective dilution number in each well with curcumin+RSL3 and curcumin+Ferrostatin-1 shown in plate 1, RSL3+Ferrostatin-1 and curcumin+RSL3+Ferrostatin-1 shown in plate 2, and the second trial of curcumin shown in plate 3

Plate 1

	1	2	3	4	5	6	7	8	9	10	11	12
A		1x	1/2x	1/4x	1/8x	1/16x	1/32x	1/64x	0x			
B		C + R	C + R	C + R	C + R	C + R	C + R	C + R	C + R	Media		
C		C + R	C + R	C + R	C + R	C + R	C + R	C + R	C + R	Media		
D		C + R	C + R	C + R	C + R	C + R	C + R	C + R	C + R	Media		
E		C + F	C + F	C + F	C + F	C + F	C + F	C + F	C + F	Media		
F		C + F	C + F	C + F	C + F	C + F	C + F	C + F	C + F	Media		
G		C + F	C + F	C + F	C + F	C + F	C + F	C + F	C + F	Media		
H												

Plate 2

	1	2	3	4	5	6	7	8	9	10	11	12
A		1x	1/2x	1/4x	1/8x	1/16x	1/32x	1/64x	0x			
B		R + F	R + F	R + F	R + F	R + F	R + F	R + F	R + F	Media		
C		R + F	R + F	R + F	R + F	R + F	R + F	R + F	R + F	Media		
D		R + F	R + F	R + F	R + F	R + F	R + F	R + F	R + F	Media		
E		C+R+F	C+R+F	C+R+F	C+R+F	C+R+F	C+R+F	C+R+F	C+R+F	Media		
F		C+R+F	C+R+F	C+R+F	C+R+F	C+R+F	C+R+F	C+R+F	C+R+F	Media		
G		C+R+F	C+R+F	C+R+F	C+R+F	C+R+F	C+R+F	C+R+F	C+R+F	Media		
H												

Plate 3

	1	2	3	4	5	6	7	8	9	10	11	12
A		1x	1/2x	1/4x	1/8x	1/16x	1/32x	1/64x	0x			
B		C	C	C	C	C	C	C	C		Media	
C		C	C	C	C	C	C	C	C		Media	
D		C	C	C	C	C	C	C	C		Media	
E												
F												
G												
H												

Key: C- curcumin; R- RSL3; F- ferrostatin-1

Once again, following 48 hours of treatment, cell viability was quantified using the WST-8 assay. We added 10 µL of reagent to each well and incubated for 1.5 hours at 37°C. Absorbance was measured at 450 nm using a microplate reader. The absorbance measurements provided insight into cell viability in each well, allowing us to assess the effectiveness of the drug combinations in killing PDAC cells.

Results

To evaluate the potential of our selected drug treatments of PDAC cells, we performed cell viability assays for each drug combination and analyzed the dose-response curves generated from the microplate reader. Monotherapy treatments were conducted for first round experiments, using curcumin, RSL3, and ferrostatin-1 as single agents. Two-drug combinations utilized all drugs and prepared every possible combination, yielding four treatment types in total. Final triple-drug dilutions combined the three drugs to act as control for the effect of RSL3, with ferrostatin-1 acting as its direct inhibitor. Cell viability was assessed after 48 hours of treatment using the WST-8 assay, and absorbance readings were analyzed to generate dose-response curves and determine half-maximal inhibitory concentrations (IC50) for each condition.
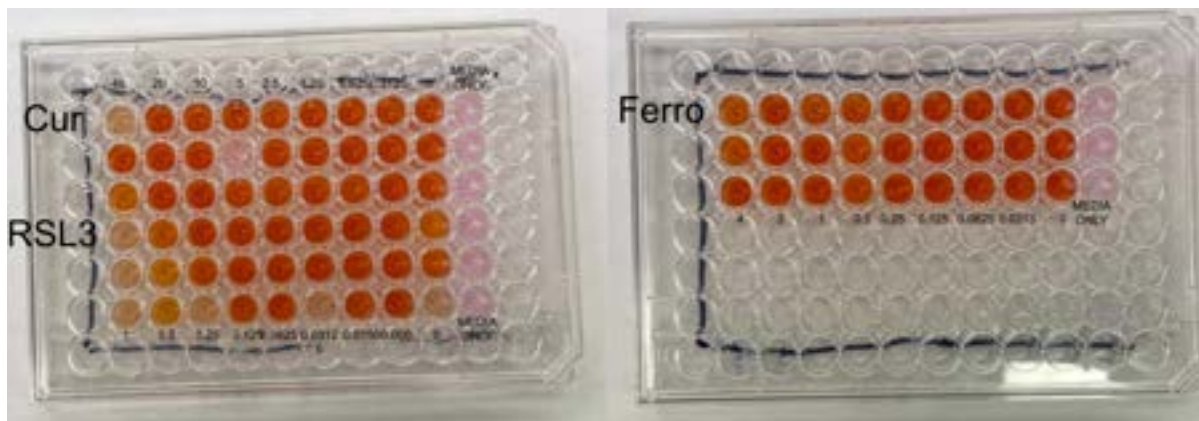
Figure 6. Cell Viability Assays for first round monotherapy drug treatments; each dilution was repeated with three replicates down the column; the molarity values (µM) are listed across the row for each specific concentration.

As shown in Figure 6, the cell viability assays for the monotherapy treatments were conducted on two 96-well plates, where 100 µL of each diluted drug treatment was added to the PDAC cells already adherent at the bottom of the plate. To create gradient scales of drug dilutions for different concentrations of drug treatment, 10 µL of WST-8 was added to each well to prepare for absorbance readings by the microplate reader. That said, the observed color gradient of the viability assays were not the most desirable, with wells that did not express an orange color at all. Well C5 stayed pink, most likely symbolizing that we didn't pipette enough WST-8 into the well while well G7 is lighter than the expected color gradient for RSL3 at its given location with a concentration of 0.03125 µM as. A lot of the wells in the G row were lighter than expected including the wells at 0.25 µM and 0 µM.
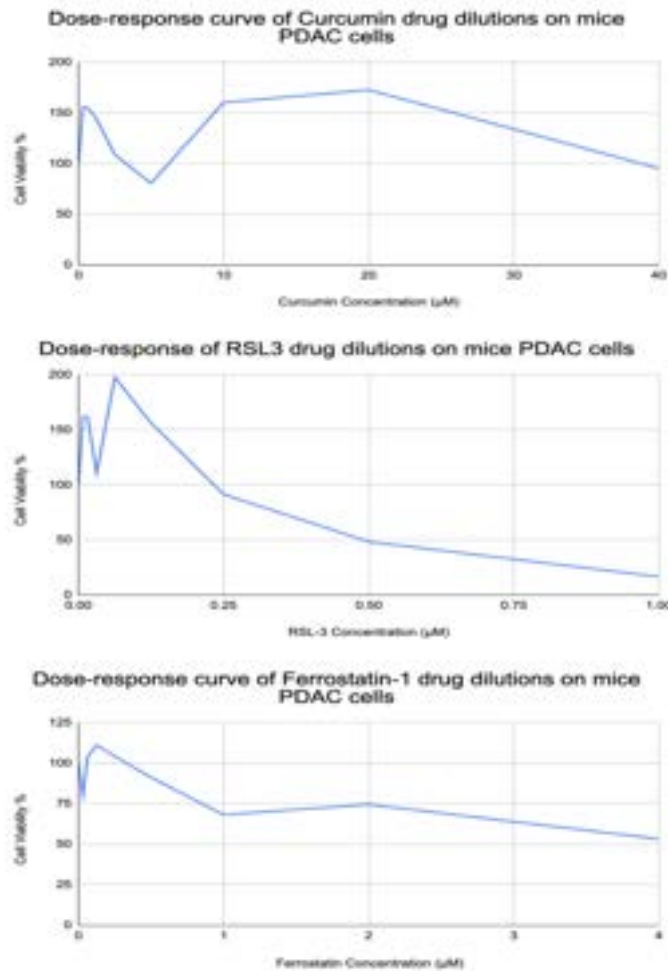
Figure 7. Graphs of dose-response curves of monotherapy drug treatments (curcumin, RSL3, ferrostatin-1)

The dose-response curves of Figure 7 from the first round monotherapy treatments demonstrate the expected overall trends in cytotoxicity, with decreasing cell viability corresponding to increasing drug concentrations, especially for RSL3. Curcumin has some varying spikes and dips throughout the graph but there is a noticeable decreasing trend towards larger concentrations. Ferrostatin cell viability decreased but not as much as that of RSL3.

The Curcumin dose-response curve showed a general decreasing trend in cell viability. However, the initial concentration range was likely underestimated, as the IC50 was not captured within the domain of the x-axis. Based on the observed trend and literature comparisons (e.g., Díaz Osterman *et al.*), the IC50 for Curcumin was estimated to be approximately 50–60 μM.
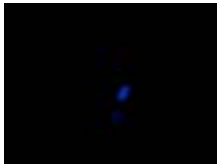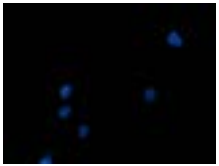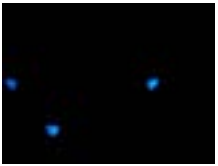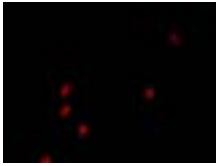
Stain\Treatment	PDAC	Curcumin	RSL3	Ferrostatin-1
Phase Contrast				
DAPI				
ROS (DCFH-DA)				

Figure 8. Images of different staining methods (Phase Contrast, DAPI, DCFH-DA) on the monotherapy drug treated/untreated cells of PDAC; images taken using fluorescent microscopy.

From our observations of IC50s following the first round of cell viability assays, we used the optimized IC50 from both dose-response curve results and predicted trend values corresponding to literature in order to treat a separate set of PDAC cells on coverslips. We used 50 μM for curcumin, 0.5 μM for RSL3, and 4 μM for ferrostatin-1 for the cover slips as well as an untreated group. We did a double stain with DAPI and DCFH-DA and viewed both under a fluorescent microscope producing the images seen in Figure 8. We can see the normal view of PDAC cells in Phase Contrast mode, the DNA from the DAPI stain under UV light, and the ROS stain under green fluorescence. The cells look shriveled compared to normal PDAc cells which are large epithelial cells.

The initial intention of this experiment was to observe and compare levels of Reactive Oxygen Species (ROS) in drug-treated cells using DCFH-DA staining, which emits green fluorescence under oxidative stress. Based on IC50 values from dose-response curves, RSL3-treated cells were expected to exhibit the highest ROS levels and brightest green fluorescence, followed by Curcumin, with Ferrostatin-1-treated cells expected to show minimal fluorescence. However, as shown in Figure 8, the stained cells instead exhibited bright red fluorescence localized around the nuclei, particularly highlighting the nucleoli.
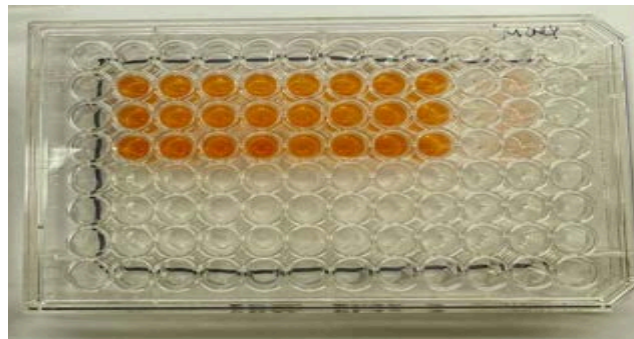
Figure 9. Cell Viability Assays for second round curcumin only drug treatment; each dilution was repeated with three replicates down the column; the molarity values (μM) are listed across the row for each specific concentration.

After the first round of monotherapy treatments, the dose response curve of Curcumin was observed to be cut off from obtaining an IC50 value, as there was a possible downward trend ending at 40 μM. Thus, a second trial was conducted for Curcumin drug dilutions starting from a higher concentration of the drug. When we ran the curcumin trial again, there was once again no noticeable difference across the color gradient of the wells. Figure 9 shows the cell viability assay that resulted from this second trial of curcumin with the gradient not being very distinguishable to the human naked eye. However, the yellow curve in Figure 10 depicts not a continued trend from 40 μM but instead a sudden rise in cell viability.
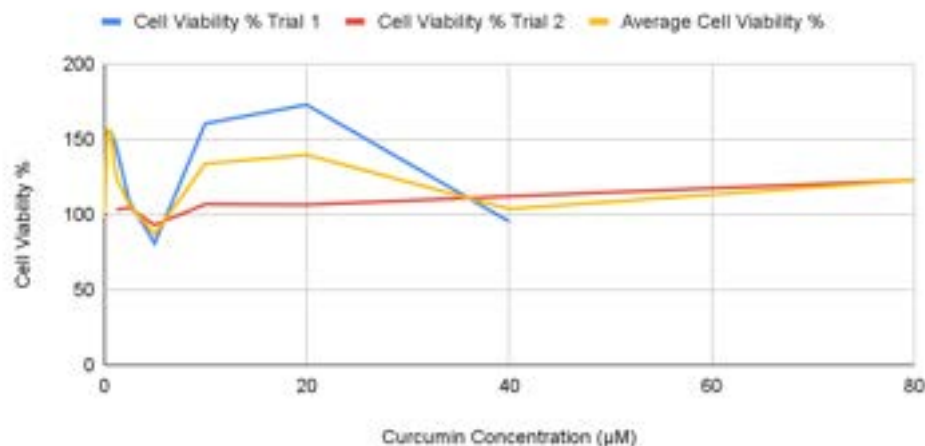

Figure 10. PDAC cells were treated with curcumin for two trials; the first trial utilized 40 μM as the starting concentration and the second trial started with 80 μM. The blue line is the cell viability from trial 1 while the orange line is from trial 2. We averaged these values we got from both trials to get the yellow line.

The IC50 values that we used for the combination trial were derived from normalized dose-response curves and aligned with established literature. The final IC50 values used for the combination experiments were determined to be 80 μM for Curcumin, 1 μM for RSL3, and 8 μM for Ferrostatin-1. We did a 2-fold serial dilution with only 7 dilutions this time due to experimental errors.
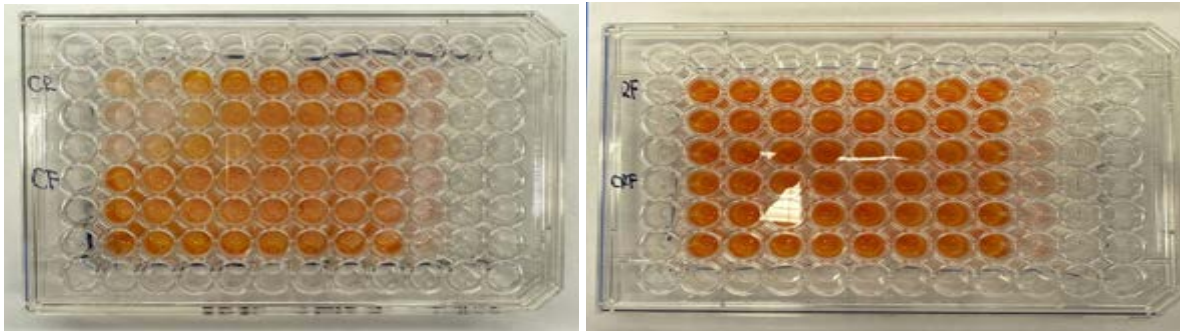

Figure 11. Cell Viability Assays for combination drug treatment; each dilution was repeated with three replicates down the column; CR stands for curcumin+RSL3, CF stands for curcumin+Ferrostatin-1, RF stands for RSL3+Ferrostatin-1, CRF stands for curcumin+RSL3+Ferrostatin-1; the molarity values (μM) are listed across the row for each specific concentration.

As shown in Figure 11, the cell viability assays for the combination treatments were conducted on two 96-well plates, where 100 μL of each diluted drug treatment was added to the PDAC cells already adherent at the bottom of the plate. To create gradient scales of drug dilutions for different concentrations of drug treatment, 10 μL of WST-8 was added to each well to prepare for absorbance readings by the microplate reader. That said, the observed color gradient of the viability assays were more desirable than the mono-drug trial, with all wells expressing an orange color. The curcumin+RSL3 trial gave the most obvious gradient where at greater concentrations of the drugs the wells are lighter shades of orange and as the concentration decreases the wells get darker. Curcumin+Ferrostatin-1, RSL3+Ferrostatin-1, and curcumin+RSL3+Ferrostatin-1 all don't have noticeable patterns or trends in gradient descent from the human eye.
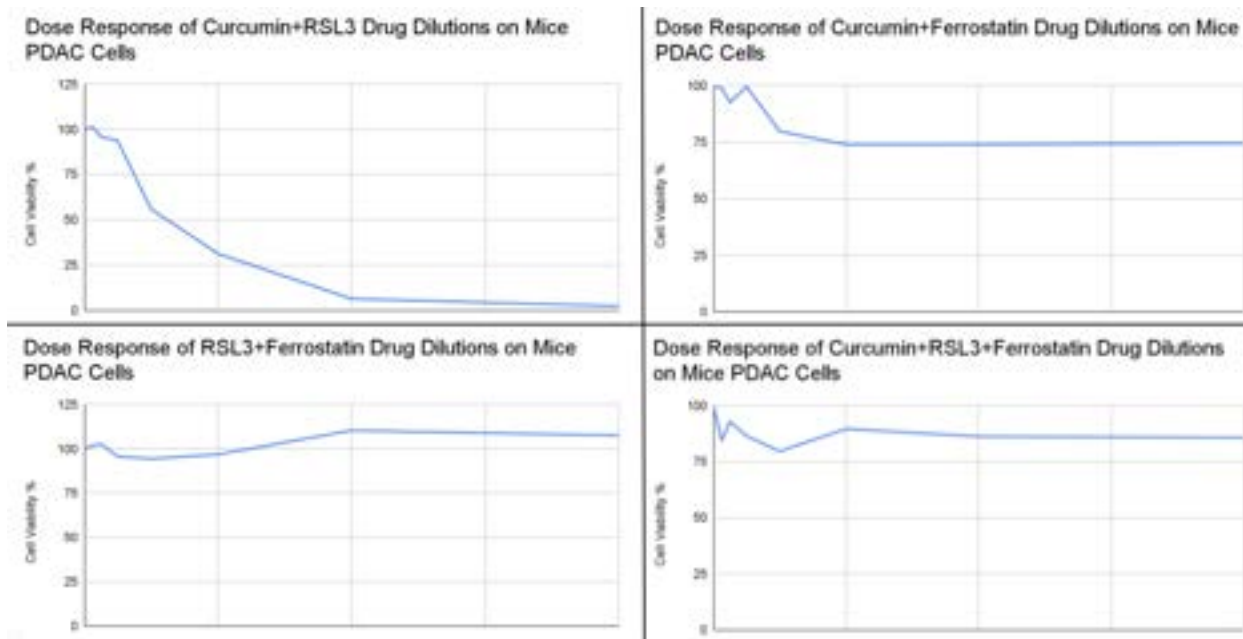
Figure 12. Graphs of dose-response curves of combination drug treatments (curcumin+RSL3, curcumin+Ferrostatin-1, RSL3+Ferrostatin-1, curcumin+RSL3+Ferrostatin-1)

The dose-response curves of Figure 12 from the second round combination treatments demonstrate the expected overall trends in cytotoxicity, with decreasing cell viability corresponding to increasing drug concentrations, especially for Curcumin+RSL3. However the other graphs don't show a noticeable decreasing trend between cell viability and drug concentrations even in combination with one another. Cell viability increases for the cells treated with RSL3+Ferrostatin-1 when all other combination drugs lead to decreasing cell viability.

Discussion

Results Analysis & Contributions

Figure 7 displays the dose-response curves and relative IC50s for monotherapeutic drug treatments. These results conform to known mechanisms and theory, where curcumin induces oxidative stress through indirect inhibition and RSL3 through direct disruption both of the GPX4 protein, which blocks liquid peroxidation. As expected, PDAC cells treated with Ferrostatin-1 should not exhibit trends of cytotoxicity, as it provokes cell proliferation; however, slight decreases in cell viability at high concentrations of Ferrostatin-1 are likely due to disruptions in cellular homeostasis or off-target effects. Evidently, RSL3 is the most effective monotherapeutic drug in inducing ferroptosis in PDAC mouse cells due to its lowest IC50 value. This is expected as Curcumin's effect on the ferroptotic pathway is more nuanced with it both inducing lipid production and also inhibiting GPX4's ability to purify these lipids. It induces ferroptosis, but not to the full extent of RSL3. Ferrostatin is normally supposed to inhibit ferroptosis by neutralizing

reactive oxygen species to increase cell viability to a certain extent. It is important to note that several data points displayed irregularities likely due to experimental errors, such as imprecise liquid handling during serial dilutions or pipetting inconsistencies when transferring treatment solutions to the 96-well plates. These unavoidable human errors may have contributed to local deviations and discrepancies in the smoothness of the curves. Despite these limitations, the general dose-response patterns remained intact, and the resulting IC50 values are consistent with concentrations reported in literature (e.g. Díaz Osterman *et al.*), especially RSL3 and Curcumin.

Interestingly, both the first and second trials of curcumin treatment exhibited nearly identical curve shapes in the lower-to-mid concentration range, including a consistent dip in cell viability near 5 μM. This reproducibility suggests that curcumin may exert its most significant cytotoxic effects at this intermediate concentration range. The consistent non-monotonic pattern, where cell viability initially decreases and then rebounds, may reflect biphasic or hormetic drug behavior, where low-to-moderate doses produce cell stress or death, but higher concentrations activate compensatory or off-target effects that restore viability or induce protective pathways.

Another plausible explanation for the increase in cell viability at higher concentrations could be solubility issues or precipitation of curcumin in aqueous media at concentrations above its solubility threshold, leading to reduced bioavailability and effective dosing. Additionally, curcumin is known to have poor stability in physiological conditions, which may further complicate interpretation of dose-response at higher doses. These results highlight the need for further optimization in curcumin delivery. Regardless of the final IC50, the data suggest curcumin may exert its strongest anti-proliferative effect around 5–10 μM in PDAC cells.

The RSL3 curve shows an overall downward trend with greater concentration of RSL3 leading to a lower PDAC cell viability. This trend however was not true across the whole data with lower concentrations of RSL3 leading to more unpredictable results. There was a spike when the RSL3 concentration was 0.0625 μM which could have been because of pipetting error or variability in cell plating density. Other possible sources of error include inconsistent mixing of the RSL3 solution, leading to uneven distribution of the drug across wells, or edge effects in the assay plate that might have influenced cell growth. The IC50 of our trial was about 0.5 μM for RSL3. When compared to other literature that used RSL3 for abdominal cancers like colorectal cancer, they achieved an IC50 of 4.085 μM but only sat them for 24 hours instead of the 48 hours like we did (Sui *et al.*, 2018). On breast cancer for 2 different cell lines, the IC50 measured at 2.668 μM and 0.5329 μM for RSL3 (Yuan *et al.*, 2025). The low IC50 suggests RSL3 could be a promising candidate for targeting GPX4-dependent pathways in PDAC.

The Ferrostatin-1 curve increased cell viability instead of decreasing it even though Ferrostatin-1 inhibits lipid peroxidation and therefore should stop ferroptosis. We expected cell

survivability to increase as ferroptosis wouldn't occur as much and therefore more cells would survive. Initially, the cell viability increases when Ferrostatin-1 is given at super small concentrations from 0.03125 μM to 0.125 μM before approximately linearly decreasing from 0.125 μM to 4 μM. This unexpected trend suggests that while low concentrations of Ferrostatin-1 may be protective and effectively inhibit ferroptosis, higher concentrations might exert cytotoxic effects due to off-target effects or cellular stress responses that get triggered from higher doses. Further experimentation, such as assessing markers of oxidative stress as well as which pathways are targeted from Ferrostatin-1 can help clarify whether the decline in viability is due to toxicity or interference with other cellular pathways. These findings highlight the importance of dose optimization when using Ferrostatin-1 as a therapeutic or experimental tool.

The goal of the cover-slip ROS stain experiment was to visually assess intracellular levels of reactive oxygen species (ROS) across the different monotherapy treatments using DCFH-DA, a commonly used ROS-sensitive fluorescent probe. Under normal conditions, DCFH-DA diffuses into live cells, where intracellular esterases cleave the acetate groups, trapping the non-fluorescent DCFH within the cytosol. In the presence of ROS, DCFH is oxidized into the fluorescent compound DCF, which emits a green signal detectable by fluorescence microscopy (excitation/emission: ~488/525 nm). Based on our IC50 results, we expected RSL3-treated cells, known to induce ferroptosis through oxidative lipid damage to exhibit the brightest green fluorescence, while curcumin-treated cells were expected to show moderate green intensity. Conversely, Ferrostatin-1, a ferroptosis inhibitor that quenches lipid peroxidation, was expected to result in minimal fluorescence due to suppressed ROS activity.

However, our microscopy results diverged from these expectations. Instead of showing green cytoplasmic fluorescence characteristic as expected from the DCFH-DA-stained cells, they displayed an abnormal red fluorescence localized near the nucleus, particularly highlighting nucleolar regions. Upon review of our protocol, we identified a critical methodological error: the cells were fixed with paraformaldehyde prior to DCFH-DA staining, rather than being stained while alive. This procedural misstep likely disrupted the dye's intended mechanism. DCFH-DA is not compatible with fixed cells, as it requires active intracellular esterases and ongoing ROS metabolism to become fluorescent. Fixation halts all cellular activity and may have led to nonspecific binding or autofluorescence, especially in dense organelles like the nucleolus, giving rise to the unexpected red staining artifact. One point worth noting is that although the stain is designed for live cells rather than fixed cells, it's unlikely that this alone would cause the stain to appear red instead of green. Additionally, instead of staining the entire cell, as reactive oxygen species (ROS) are typically distributed throughout, it only stains the nucleolar region, which is also unexpected.

Thus, the misleading fluorescence observed in Figure 8 could be because of a post-fixation staining, which rendered the ROS detection protocol ineffective though very unlikely due to the change in color and region the new stain exists in. Future attempts to visualize ROS with DCFH-DA should strictly involve live-cell staining protocols, or adjust the fixation method using methanol instead of paraformaldehyde to create an environment for ROS formation (Shen et al.). This correction would ensure the proper assessment of oxidative stress levels induced by each treatment.

For the combinatorial drug trial as depicted in Figure 12, the combination of Curcumin and RSL3 exhibited the most pronounced cytotoxic effect, with cell viability dropping below 10% at higher concentrations, which may indicate a possible strong synergistic induction of ferroptosis. Due to the fact we used store-bought curcumin and not pure pharmaceutical pure curcumin, the resulting concentration of RSL3 on its own and RSL3+curcumin and their respective IC50 don't vary by much. Investigations using purer curcumin should be used to see if the IC50 value of RSL3+curcumin concentration will decrease compared to RSL3 on its own.

In contrast, treatments involving Curcumin + Ferrostatin-1 and RSL3 + Ferrostatin-1 maintained consistently high cell viability (~80–100%), confirming Ferrostatin-1's protective role against lipid peroxidation-driven cell death. Similarly, in the triple treatment (Curcumin + RSL3 + Ferrostatin-1), cell viability remained high and stable, further validating that Ferrostatin-1 effectively neutralizes the ferroptotic effects of both agents. The stark contrast between the steep decline in the Curcumin + RSL3 curve and the flat trends observed in the other combinations underscores that the observed cell death is specifically ferroptotic, rather than a result of off-target toxicity. These results highlight the therapeutic relevance of targeting GPX4 and lipid peroxidation in PDAC, and underscore the value of Ferrostatin-1 as a mechanistic control. Overall, the findings support the potential of combinatorial therapies involving ferroptosis inducers for PDAC treatment, with Ferrostatin-1 serving as a critical tool to confirm pathway specificity.

Limitations
One key limitation of our study is that we conducted only a single trial for each IC50 assay across all treatment conditions, including monotherapy, two-drug combinations, and the three-drug treatment. This limited number of independent trials restricts our ability to account for variability between experiments and introduces potential bias in the resulting data. Consequently, the reproducibility and robustness of our findings are somewhat constrained.

However, it is important to note that within each assay, all drug concentrations were tested through three experimental replicates on the 96-well plate using a microplate reader to generate dose-response curves and calculate IC50 values. These replicates help reduce variability due to pipetting or cell seeding inconsistencies at the well level and improve the reliability of individual

measurements. Nonetheless, future studies should include biological replicates, repeated independent experiments, to strengthen the validity of the results and allow for statistical significance testing.

Another limitation of our study is the use of a mouse PDAC cell line, which can not for sure represent the biological complexity of human PDAC. While mouse models provide valuable insights into cancer mechanisms and allow for controlled experimental conditions, they differ from human tumors in genetic makeup and therefore drug response. As a result, these findings we got from mouse PDAC cells may not directly translate to human clinical settings. Our experiments were conducted in vitro, without in vivo validation, which limits the assessment of ferroptosis within the complex tumor microenvironment. Also, the use of a single cell line means that our results do not capture all the complexities that PDAC may have.

Furthermore, while we measured lipid peroxidation as a marker of ferroptosis, other markers and methods like using lipidomics would provide greater insights. Finally, we did not evaluate immune-related effects or tumor immune interactions, both of which are important in understanding this therapeutic potential of ferroptosis in PDAC mouse cells.

Future Directions

From our results, we were able to conclude superior performance from drug combinatorial treatments against PDAC cells, specifically utilizing the natural compound, curcumin, along with the ferroptosis inducer RSL3. As previously mentioned, our study was flawed in its experimental design and failed to include biological replicates of all IC50 and dose-response experiments. Repeating these trials independently would help validate our findings more authentically through reducing experimental bias and enabling robust analysis of the treatment effects. Furthermore, molecular studies that allow visualization of gene expression should be performed. Techniques such as qPCR, western blotting, or even RNA sequencing could be used to analyze the expression of key genes and proteins involved in programmed cell death, further validating RSL3 and curcumin's ability to induce ferroptosis. Nevertheless, Ferrostatin-1 was utilized in the present study to act as confirmation for the mode of cell death through specifically inhibiting the function of RSL3, which strengthens the theoretical pathway deduced.

Long-term goals would include in vivo validation of our effective drug combinations using mouse models of PDAC, such as xenografts. These studies are the cornerstone to practical implementations in therapeutic environments, as they evaluate not only treatment efficacy but also potential toxicity risks apparent in a whole organism.

Additional exploration could also include dosage optimization using models like the Chou-Talalay method in order to determine most effective drug ratios with minimal toxicity. Regarding this, other investigations for potential drug resistance by exposing PDAC cells to

long-term treatment and examining changes in gene expression or sensitivity to therapy would also provide valuable insights for informed therapeutic planning.

Conclusion

In conclusion, our study highlights the potential of RSL3 and curcumin as effective inducers of ferroptosis in PDAC, with RSL3 demonstrating the strongest cytotoxic effect. While initial results support the viability of combinatorial treatments targeting oxidative stress pathways, technical limitations such as lack of biological replicates and errors in ROS visualization cause the need for further validation. Future work incorporating molecular analysis, live-cell imaging, and in vivo testing will be essential to confirm these findings and advance ferroptosis-based strategies for treating PDAC.

References

1. Al-Lazikani, B., Banerji, U., & Workman, P. (2012). Combinatorial drug therapy for cancer in the post-genomic era. Nature biotechnology, 30(7), 679–692. https://doi.org/10.1038/nbt.2284

2. Ayala, A., Muñoz, M. F., & Argüelles, S. (2014). Lipid peroxidation: production, metabolism, and signaling mechanisms of malondialdehyde and 4-hydroxy-2-nonenal. Oxidative medicine and cellular longevity, 2014, 360438. https://doi.org/10.1155/2014/360438

3. Díaz Osterman, C. J., Gonda, A., Stiff, T., Sigaran, U., Valenzuela, M. M., Ferguson Bennit, H. R., Moyron, R. B., Khan, S., & Wall, N. R. (2016). Curcumin Induces Pancreatic Adenocarcinoma Cell Death Via Reduction of the Inhibitors of Apoptosis. Pancreas, 45(1), 101–109. https://doi.org/10.1097/MPA.0000000000000411

4. Dixon, S. J., Lemberg, K. M., Lamprecht, M. R., Skouta, R., Zaitsev, E. M., Gleason, C. E., Patel, D. N., Bauer, A. J., Cantley, A. M., Yang, W. S., Morrison, B., 3rd, & Stockwell, B. R. (2012). Ferroptosis: an iron-dependent form of nonapoptotic cell death. Cell, 149(5), 1060–1072. https://doi.org/10.1016/j.cell.2012.03.042

5. Gorrini, C., & Mak, T. W. (2019). Glutathione Metabolism: An Achilles' Heel of ARID1A-Deficient Tumors. Cancer cell, 35(2), 161–163. https://doi.org/10.1016/j.ccell.2019.01.017

6. Guo, Z., Zhuang, H., & Shi, X. (2024). Therapeutic efficacy of ferroptosis in the treatment of colorectal cancer (Review). Oncology letters, 28(6), 563. https://doi.org/10.3892/ol.2024.14697

7. Jiang, Y., Hui, D., Pan, Z. et al. Curcumin promotes ferroptosis in hepatocellular carcinoma via upregulation of ACSL4. J Cancer Res Clin Oncol 150, 429 (2024). https://doi.org/10.1007/s00432-024-05878-0

8. Kim, H., & Xue, X. (2020). Detection of Total Reactive Oxygen Species in Adherent Cells by 2',7'-Dichlorodihydrofluorescein Diacetate Staining. Journal of visualized experiments : JoVE, (160), 10.3791/60682. https://doi.org/10.3791/60682

9. Lopez-Blazquez, C., Lacalle-Gonzalez, C., Sanz-Criado, L., Ochieng' Otieno, M., Garcia-Foncillas, J., & Martinez-Useros, J. (2023). Iron-Dependent Cell Death: A New Treatment Approach against Pancreatic Ductal Adenocarcinoma. International journal of molecular sciences, 24(19), 14979. https://doi.org/10.3390/ijms241914979

10. Perera, L., Brown, S. M., Silver, B. B., Tokar, E. J., & Sinha, B. K. (2025). Ferroptosis Inducers Erastin and RSL3 Enhance Adriamycin and Topotecan Sensitivity in ABCB1/ABCG2-Expressing Tumor Cells. International Journal of Molecular Sciences, 26(2), 635. https://doi.org/10.3390/ijms26020635

11. Sarantis, P., Koustas, E., Papadimitropoulou, A., Papavassiliou, A. G., & Karamouzis, M. V. (2020). Pancreatic ductal adenocarcinoma: Treatment hurdles, tumor microenvironment and immunotherapy. World journal of gastrointestinal oncology, 12(2), 173–181. https://doi.org/10.4251/wjgo.v12.i2.173

12. Shen, W. J., Hsieh, C. Y., Chen, C. L., Yang, K. C., Ma, C. T., Choi, P. C., & Lin, C. F. (2013). A modified fixed staining method for the simultaneous measurement of reactive oxygen species and oxidative responses. Biochemical and biophysical research communications, 430(1), 442–447. https://doi.org/10.1016/j.bbrc.2012.11.037

13. Siegel, R. L., Giaquinto, A. N., & Jemal, A. (2024). Cancer statistics, 2024. CA: a cancer journal for clinicians, 74(1), 12–49. https://doi.org/10.3322/caac.21820

14. Stoffel, E. M., Brand, R. E., & Goggins, M. (2023). Pancreatic Cancer: Changing Epidemiology and New Approaches to Risk Assessment, Early Detection, and Prevention. Gastroenterology, 164(5), 752–765. https://doi.org/10.1053/j.gastro.2023.02.012

15. Sui, X., Zhang, R., Liu, S., Duan, T., Zhai, L., Zhang, M., Han, X., Xiang, Y., Huang, X., Lin, H., & Xie, T. (2018). RSL3 Drives Ferroptosis Through GPX4 Inactivation and ROS Production in Colorectal Cancer. Frontiers in pharmacology, 9, 1371. https://doi.org/10.3389/fphar.2018.01371

16. Sun, S., Shen, J., Jiang, J. et al. Targeting ferroptosis opens new avenues for the development of novel therapeutics. Sig Transduct Target Ther 8, 372 (2023). https://doi.org/10.1038/s41392-023-01606-1

17. Tang, X., Ding, H., Liang, M., Chen, X., Yan, Y., Wan, N., Chen, Q., Zhang, J., & Cao, J. (2021). Curcumin induces ferroptosis in non‐small‐cell lung cancer via activating autophagy. Thoracic Cancer, 12(8), 1219–1230. https://doi.org/10.1111/1759-7714.13904

18. Valsecchi, M.E., Díaz-Cantón, E., de la Vega, M. et al. Recent Treatment Advances and Novel Therapies in Pancreas Cancer: A Review. J Gastrointest Canc 45, 190–201 (2014). https://doi.org/10.1007/s12029-013-9561-z

19. Yang, W. S., SriRamaratnam, R., Welsch, M. E., Shimada, K., Skouta, R., Viswanathan, V. S., Cheah, J. H., Clemons, P. A., Shamji, A. F., Clish, C. B., Brown, L. M., Girotti, A. W., Cornish, V. W., Schreiber, S. L., & Stockwell, B. R. (2014). Regulation of ferroptotic cancer cell death by GPX4. Cell, 156(1-2), 317– 331. https://doi.org/10.1016/j.cell.2013.12.010

20. Yesilkanal, A. E., Johnson, G. L., Ramos, A. F., & Rosner, M. R. (2021). New strategies for targeting kinase networks in cancer. The Journal of biological chemistry, 297(4), 101128. https://doi.org/10.1016/j.jbc.2021.101128

21. Yuan, J., Liu, C., Jiang, C., Liu, N., Yang, Z., & Xing, H. (2025). RSL3 induces ferroptosis by activating the NF-κB signalling pathway to enhance the chemosensitivity of triple-negative breast cancer cells to paclitaxel. Scientific reports, 15(1), 1654. https://doi.org/10.1038/s41598-025-85774-w

22. Zhang, L.; Sanagapalli, S.; Stoita, A. Challenges in Diagnosis of Pancreatic Cancer. World J. Gastroenterol. 2018, 24 (19), 2047–2060. https://doi.org/10.3748/wjg.v24.i19.2047

23. Zhou, Q., Meng, Y., Li, D. et al. Ferroptosis in cancer: from molecular mechanisms to therapeutic strategies. Sig Transduct Target Ther 9, 55 (2024). https://doi.org/10.1038/s41392-024-01769-5